

Design of a Multi-Band U-Slot Microstrip Patch Antenna

Ahmed Samir^{1,3*}, Ahmed Fawzy^{2*}, Hala M. Abd El Kader³

¹MTI University, Department of Communications Engineering, Egypt

²Nanotechnology Central Lab, Electronics Research Institute, El Tahrir St., Giza, Egypt.

³Electrical Engineering Department, Faculty of Engineering (Shoubra), Banha University, Egypt

Abstract: This paper presents multiband U slot rectifying antenna in RF energy harvesting system. The difference between two microstrip patch antennas for energy harvesting system from surrounding RF signals at several frequencies is proposed. The first one is single band antennas at three frequencies 2 GHz, 3.7 GHz and 5.8 GHz. The second one is a compact antenna which operates at the same frequencies at the same time. The design, simulation and fabrication of the proposed antennas were performed. The design of a multiband antenna is based on U-slots shapes. Furthermore, the paper presents RF-DC rectifier using the Agilent diode HSMS-2850 and advanced design system (ADS) simulator. The antenna operates at multi-band frequencies such as GPS band, Wi-Fi band, and Wi-Max band with reflection coefficient below -20 dB. The proposed RF energy harvester system will allow collecting power as much as possible at the desired frequencies. It is very effective in many applications that don't need high power consumption like wireless sensor networks (WSN).

Keywords: Energy harvesting, Microstrip antenna, Rectifier circuits, Multiband antenna.

Date of Submission: 04-12-2019

Date of Acceptance: 19-12-2019

I. Introduction

Nowadays, with the rapid development of wireless communication systems, wireless sensor network nodes have been attracting most of researchers. The main requirement for design of these devices is the power consumption. Batteries are the power source of these devices, but the life time of the network nodes is limited by the batteries capacity. So the RF energy harvesting system is one of the solutions of this problem. Energy harvesting means that converting the electromagnetic waves around us radiated from many sources such as cellular mobile communications, Wi-Fi, Bluetooth, Television, and Radio waves into positive power for these devices [1-2]. Therefore, RF energy harvesting have attracted significant attention in the past few years [3-4]. A rectifying antenna is one of the most popular devices for harvesting applications. Several works have been made [5-8]. Multiband antennas are promising solution to harvest RF power from different sources and from different channels simultaneously to DC power. In this work, a multiband antenna is proposed and designed for energy harvesting application. A comparison between single frequency antenna and multiband antenna has been made. The comparison showed that the multiband antenna has small size and wider bandwidth. Performance improvement is happened by using U slot multiband antenna instead of single frequency antenna.

II. Microstrip Patch Antenna Design Process

The essential parameters for the design of a rectangular microstrip patch antenna are:

1. Calculation of patch width (W)

$$W = \frac{1}{2f_r \sqrt{\mu_0 \epsilon_0}} \sqrt{\frac{2}{\epsilon_r + 1}} = \frac{c}{2f_r} \sqrt{\frac{2}{\epsilon_r + 1}} \quad (1)$$

Where c is the free space velocity of light, ϵ_r is dielectric constant of substrate and f_r is the operating frequency.

2. Calculation of effective dielectric constant (ϵ_{reff})

$$\epsilon_{\text{reff}} = \frac{\epsilon_r + 1}{2} + \frac{\epsilon_r - 1}{2} \left[1 + 12 \frac{h}{W} \right]^{-1/2} \quad (2)$$

The effective dielectric constant of the rectangular microstrip patch antenna treats the antenna as if all the fields were contained within a humongous substrate [7-9].

3. Calculation extension length (ΔL)

$$\Delta L = 0.412 \times h \times \frac{(\epsilon_{\text{eff}} + 0.3) \left(\frac{W}{h} + 0.264 \right)}{(\epsilon_{\text{eff}} - 0.258) \left(\frac{W}{h} + 0.8 \right)} \quad (3)$$

The extension length is used for calculating resonant frequency of microstrip antenna.

4. Calculation of the effective length (L_{eff}) & actual patch length (L)

$$L_{\text{eff}} = \frac{1}{2 f_r \sqrt{\epsilon_{\text{eff}} \sqrt{\mu_0 \epsilon_0}}} \quad (4)$$

$$L = L_{\text{eff}} - 2\Delta L \quad (5)$$

2.1 Rogers duroid 5880 substratematerial

For a patch antenna designed using 1.575 mm, Rogers duroid 5880 material with a relative permittivity of 2.2 works at three frequencies, 2.5 GHz, 3.7 GHz and 5.8 GHz. The design consideration is how to take energy to the patch. The coaxial feed is the feed technique which used due to its simple in design in spite of its narrow bandwidth [16-24]. The key point in using a coaxial feed is where it should be located on the patch in order to achieve the desired input impedance for matching. With the coaxial feed at the midpoint of the width of the patch and the input impedance of the patch can be tuned by adjusting the location of the feed point relative to the center of the patch. Note that the patch input impedance decreases as the feed point moves towards the center and the inverse case is occurs when moves towards the edge [10-11]. The dimensions of the coaxial cable should be calculated to achieve the correct characteristic impedance Z_0 . The dimensions of coaxial cable consist of the radius of the pin (a) and the radius of the ground shield (b). For a cable 1m along, the inductance and capacitance parameters are given by

$$L = \frac{\mu}{2\pi} \ln \frac{b}{a} \quad (6)$$

$$C = \frac{2\pi\epsilon}{\ln \frac{b}{a}} \quad (7)$$

Where μ is the permeability and ϵ is the real part of permittivity of the insulator between the conductors. The Characteristic impedance Z_0 can calculate by

$$Z_0 = \sqrt{\frac{L}{C}} \quad (8)$$

For a lossless transmission line, the ratio of $\frac{b}{a}$ can be calculated by

$$\frac{b}{a} = e^{2\pi Z_0 \sqrt{\frac{\mu}{\epsilon}}} \quad (9)$$

The first consideration in simulation setup is specifying the solution type. In this case, "Model" was selected for solution type. According to simulation documentation, the "Model" solution type is desirable for simulating passive and high frequency patches for calculating the S- parameters using reflected and incident powers. The second consideration in simulation setup was the patch excitation. "Lumped Port" was used as a patch excitation [6-12]. This was achieved by drawing a circle equal to the diameter of the coaxial ground shield and placing it at the end of the connector. The integration line for the excitation was connected from the pin to the ground shield. The "Lumped Port" excitation is choosing in order to its serves as a mechanism, such as a lumped impedance or source that can be used for S-parameter measurement or for excitation that is analogy to exciting or measuring a transmission line. The third consideration in simulation setup was to create a box centered around the patch and wide enough so that the distance between the patch surface and the box edge is at least 0.125 wavelengths [19-21]. This box was assigned to be as a vacuum. The location of the feed point not only affects the input impedance of the patch, but also it influences the resulting resonant frequency. This means that the patch dimension and the feed point must be chosen together to optimize the patch design and get the best patch dimensions [17-23].

2.2 Parametric study at 2GHz

The parametric study performed a sweep over the length, width and the feed offset from edge. The length was varied from 44 mm to 49 mm with increments of 0.5 mm, the width was varied from 49 mm to 53 mm with increments of 0.5mm, and the feed offset was varied from 6 mm to 12 mm with increments of 1 mm. The performance of each simulation was judged by the magnitude of S11 and the resonant frequency Figure-1 illustrates the results of this study. The result of this study is a patch design that operates at 2 GHz with a reflection coefficient of -40.1587 dB .The dimensions of this patch are 46.5 mm for the length, 50.5 mm for the width, and a feed offset of 8 mm.

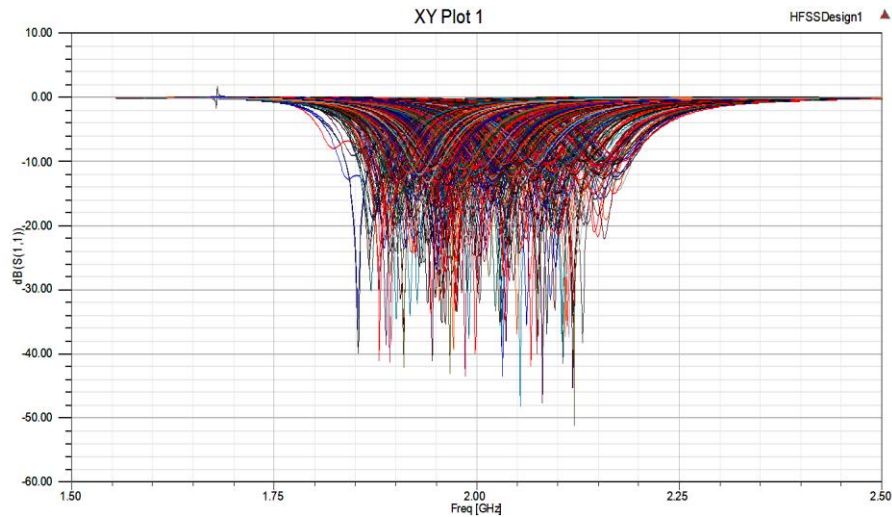


Fig 1. Magnitude of S_{11} for the final patch design at 2 GHz

2.3 Parametric study at 3.7 GHz

The parametric study performed a sweep over the length, width and the feed offset from edge. The length was varied from 23 mm to 27 mm with increments of 0.5 mm, the width was varied from 23 mm to 27 mm with increments of 0.5mm, and the feed offset was varied from 2 mm to 6 mm with increments of 0.5 mm.

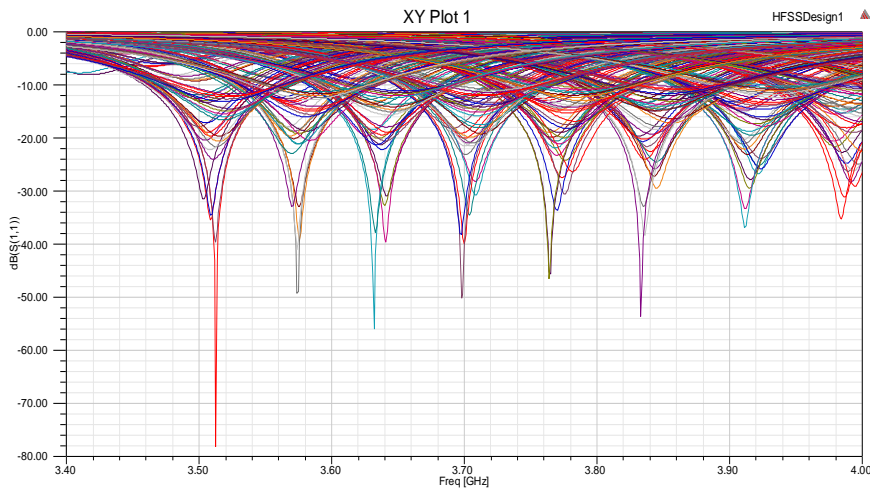


Fig 2. Magnitude of S_{11} for the final patch design at 3.7GHz

The performance of each simulation was judged by the magnitude of S_{11} and the resonant frequency Figure-2 illustrates the results of this study. The result of this study is a patch design that operates at 3.7 GHz with a reflection coefficient of -40.15 dB. The dimensions of this patch are 25.5 mm for the length, 25 mm for the width, and a feed offset of 4.5 mm.

2.4 Parametric study at 5.8 GHz

The parametric study performed a sweep over the length, width and the feed offset from edge. The length was varied from 13 mm to 22 mm with increments of 1 mm, the width was varied from 18 mm to 25 mm with increments of 1mm, and the feed offset was varied from 3 mm to 8 mm with increments of 1 mm. The performance of each simulation was judged by the magnitude of S_{11} and the resonant frequency Figure-3 illustrates the results of this study.

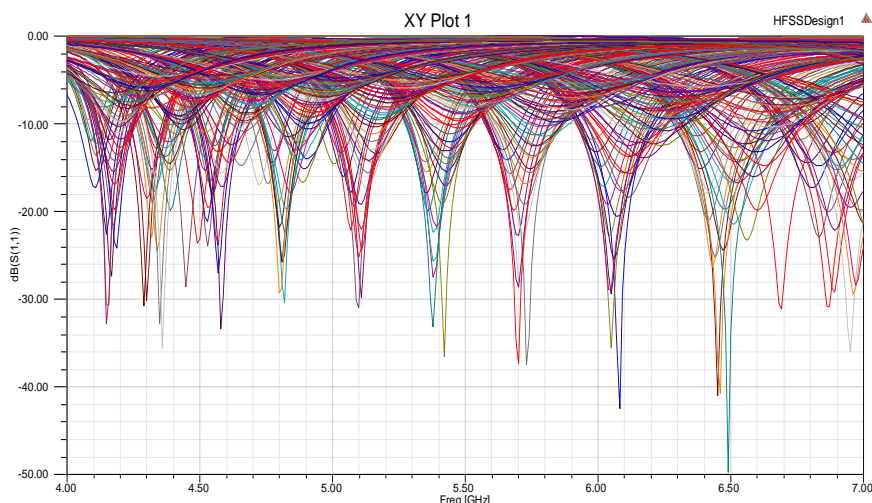


Fig 3. Magnitude of S₁₁ for the final patch design at 5.8 GHz

The result of this study is a patch design that operates at 5.8 GHz with a reflection coefficient of -37.5115 dB. The dimensions of this patch are 16 mm for the length, 18 mm for the width, and a feed offset of 3 mm. Finally, the microstrip patch antenna design for several frequencies 2 GHz, 3.7 GHz and 5.8 GHz respectively is concluded the table no 1 and for each frequency the optimal patch dimension, the optimal feed point and also the magnitude of reflection coefficient S₁₁ is shown in the table.

Table no 1: The conclusion results for the designed patch antenna at the operated frequencies.

The operating Frequency	The optimal Patch Dimensions (mm)		The Optimal Feed Offset Point	Reflection Coefficient (S ₁₁)
	Width	Length		
2 GHz	50.5	46.5	8	-40.1587 dB
3.7 GHz	25	25.5	4.5	-40.1501 dB
5.8 GHz	18	16	3	-37.5115 dB

III. U-slot antenna design

The design of the proposed antenna is shown in Figure-4 while geometric dimensions are listed in Table no2. This antenna consists of coplanar monopole that collects large amount of Electromagnetic signals from several communication bands. The topology of the antenna is designed on FR4 epoxy material with thickness (H) 1.6 mm, dielectric constant of 4.4 and loss tangent of 0.02. The overall dimensions of the antenna are 65 × 70 × 1.6 mm². Three U-Slots are used for multi band antenna and H-Slot offers better flexibility [14-22]. In the proposal antenna, we used FR4 material instead of Rogers's duroid 5880 because FR4 materials have a lot of advantages such as electrical insulators with high dielectric strength, light weight and low cost. The proposed antenna can be used for WCDMA/Wi-MAX/Wi-Fi bands. In this section, we will show all simulation results for the proposed antenna as shown in the following figures.

Table no 2: The proposed antenna dimensions (mm).

L	W	T	H	W1
65	70	0.5	1.6	10
W2	W3	W4	W5	W6
2	3	8	5	12
W7	L1	L2	L3	L4
15	16	10	20	45

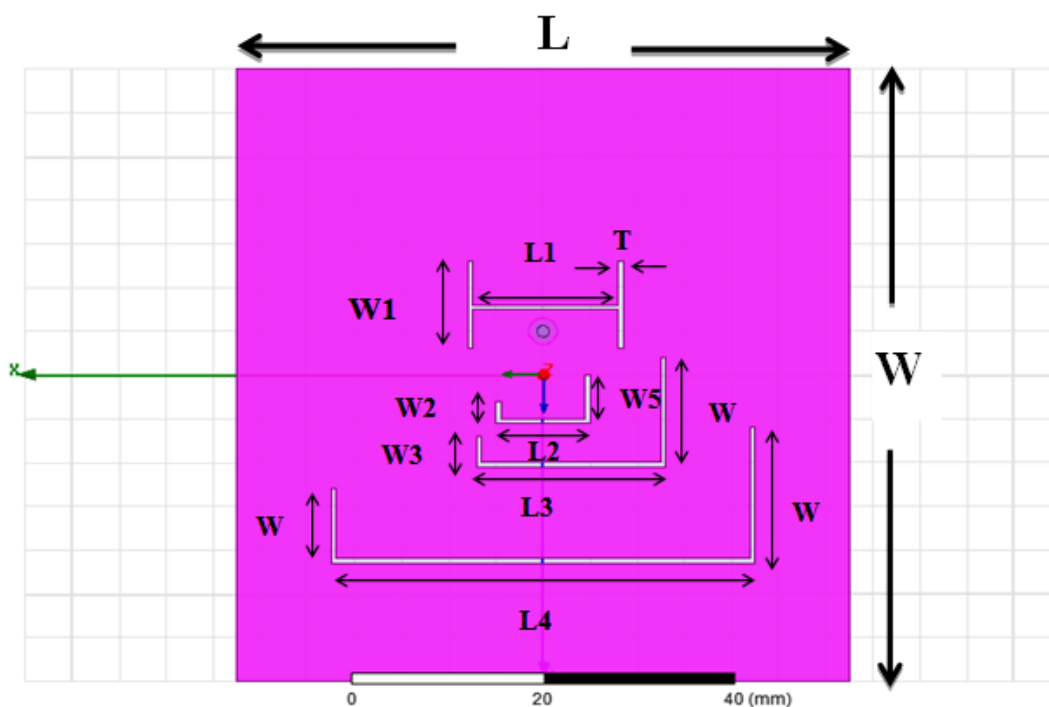


Fig 4. Geometrical Configuration of the proposed antenna

3.1 Return loss

Return loss (S_{11}) is very good for all frequencies where the values at 2 GHz, 3.7 GHz and 5.8 GHz are -15.75 dB, -15.21dB and -15.73 dB respectively, as shown in Figure-5.

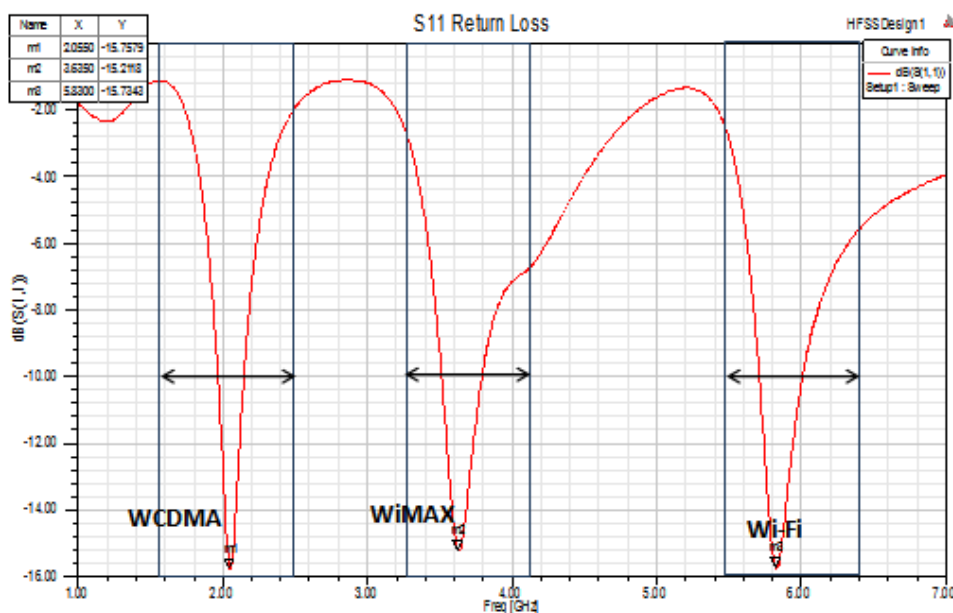
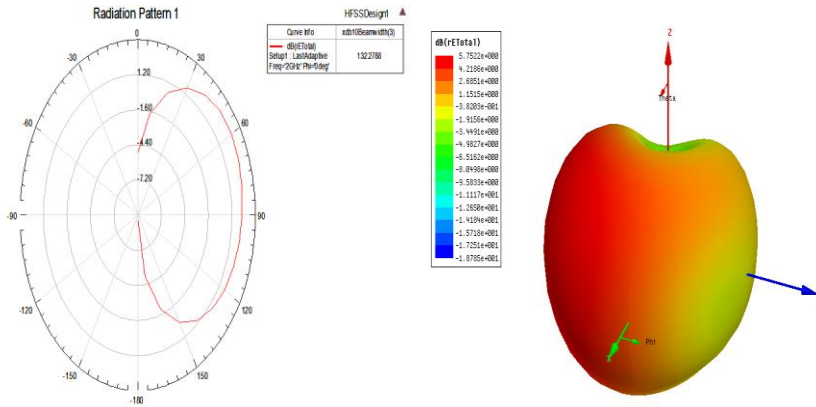


Fig 5. Return loss results of the proposed antenna

3.2 Radiation pattern and 3-D polargain

Antenna radiation patterns are simulated at one frequency, one polarization, and one plane cut. The patterns are usually presented in polar or rectilinear form with a dB strength scale. Since a Microstrip patch antenna radiates broadband patch surface, the elevation pattern for $\phi = 0$ degree would be important and also antenna radiation pattern gain are shown in Figure-6 and Figure-7 respectively.



(a) 2-D Radiation Pattern (b) 3-D Radiation Pattern
Fig 6. (a) 2-D Radiation Pattern and (b) 3-D Radiation Pattern

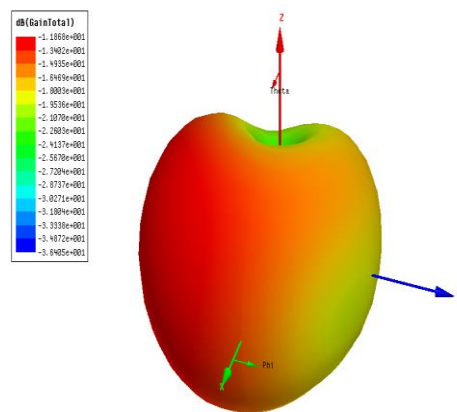


Fig 7. 3-D Polar Gain of the proposed antenna

3.3 Voltage standing wave ratio (VSWR)

The most common case for measuring VSWR is when installing and tuning transmitting antennas. When a transmitter is connected to an antenna by a feed line, the impedance of the antenna and feed line must be exactly for maximum energy transfer from the feed line to the antenna to be possible. When an antenna and feed line do not have matching impedances, some of electrical energy cannot be transferred from the feed line to the antenna. Energy not transferred to the antenna is reflected back towards the transmitter. It is the interaction of these reflected waves with forward waves which causes standing wave pattern as shown in Figure-8. Ideally, VSWR must lie in the range of 1-2 for achieved good impedance matching. For the frequency 2 GHz, VSWR = 1.3976, for the frequency 3.7 GHz, VSWR = 1.4203 and for the frequency 5.8 GHz, VSWR = 1.4009.

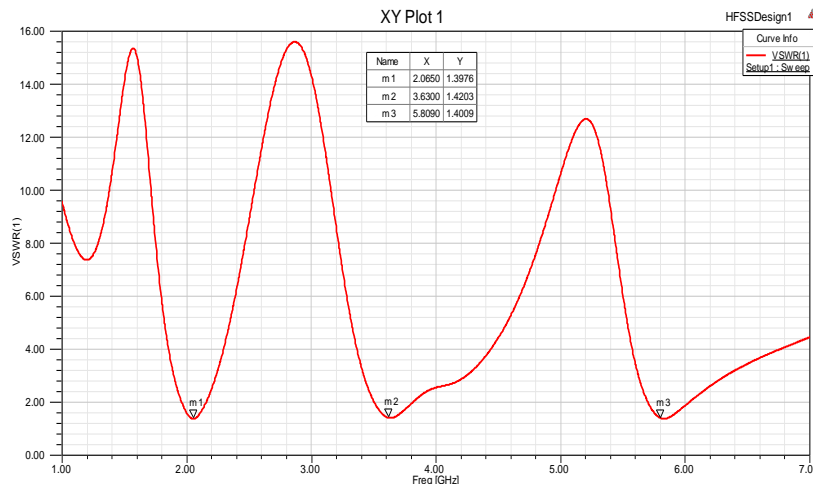


Fig 8. Voltage Standing Wave Ratio (VSWR) of the proposed antenna

3.4 Antennabandwidth

The bandwidth is the difference between upper frequency and lower frequency around the resonance frequency at -10 dB. The fractional bandwidth was calculated by the equation (10) for all resonance frequencies to determine if the antenna still operates in UWB range, as shown in Figure-9.

$$B.W_f = 2 \left(\frac{f_{up} - f_{low}}{f_{up} + f_{low}} \right) \times 100\% \quad (10)$$

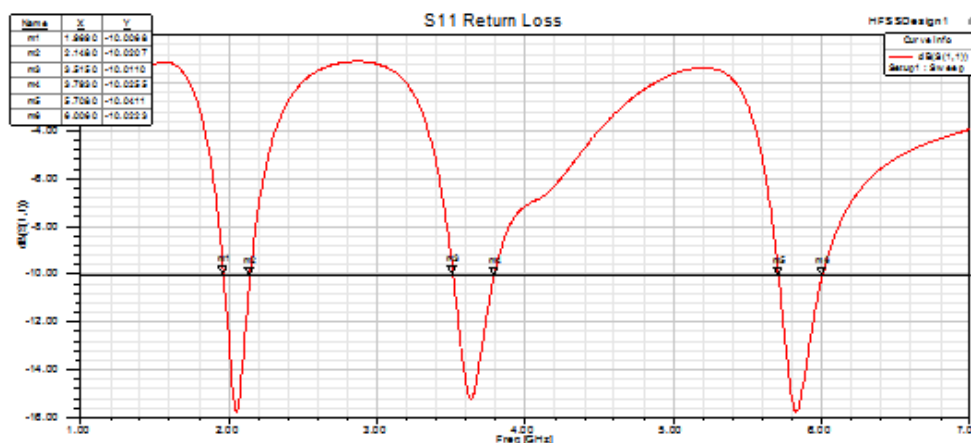


Fig 9. Bandwidth results of the proposed antenna

At 2 GHz, upper frequency is 2.148 GHz and lower frequency is 1.969 GHz then the Bandwidth is 179 MHz and $B.W_f = 8.7\%$, At 3.7 GHz, upper frequency is 3.793 GHz and lower frequency is 3.515 GHz then the Bandwidth is 278 MHz and $B.W_f = 7.6\%$ and At 5.8 GHz, upper frequency is 6.006 GHz and lower frequency is 5.708 GHz then the Bandwidth is 298 MHz and $B.W_f = 5.1\%$.

3.5 Electric field and magnetic field patterns

Figure-10 and Figure-11 presents variation in current distribution in E-Field and H-Field of the antenna. Where the maximum value of E-Field of the proposed antenna is $1.6219e+004$ which has the red color and also the maximum value of H-Field of the proposed antenna is $7.1212e+001$ in red color.

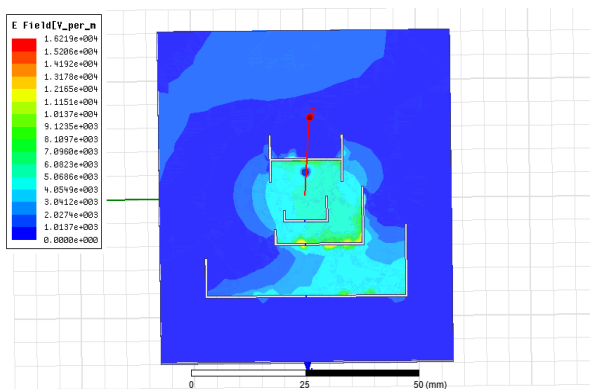


Fig 10. Electric Field Pattern of the proposed antenna

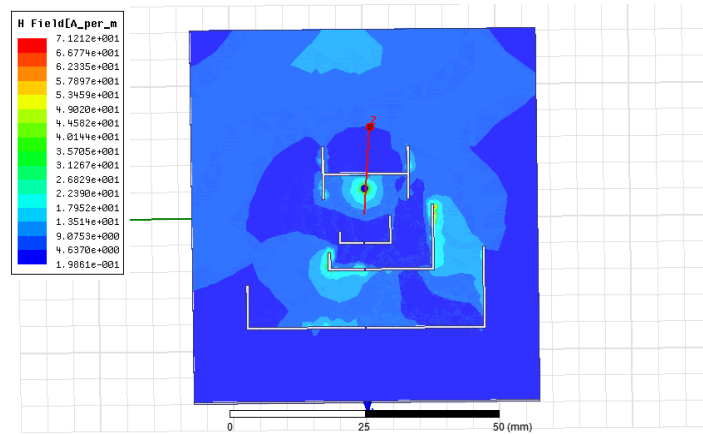


Fig 11. Magnetic Field Pattern of the proposed antenna

IV. Antenna fabrication and measurement data

The proposed antenna has been fabricated by PCB technique and tested by vector network analyzer on FR4 double sided PCB material as shown in Figure-12 and Figure-13.

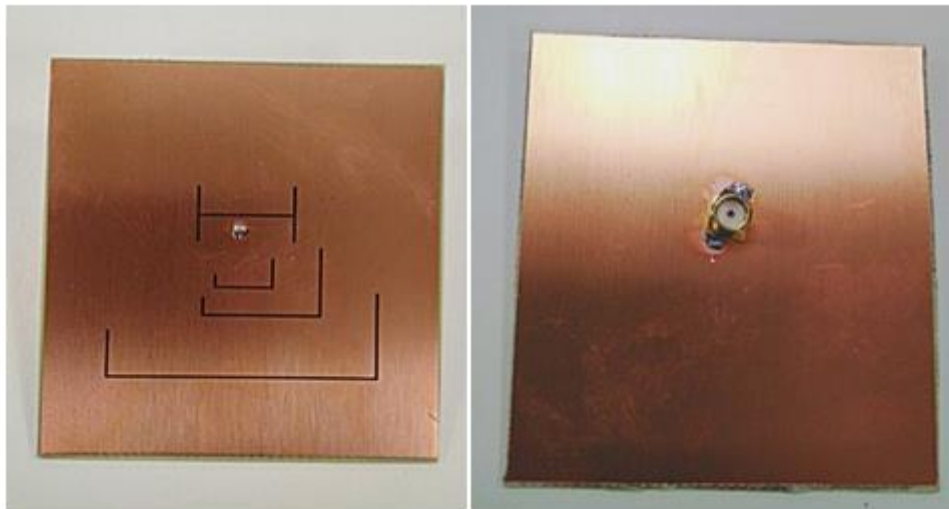


Fig 12. Front view and rear view of proposed antenna

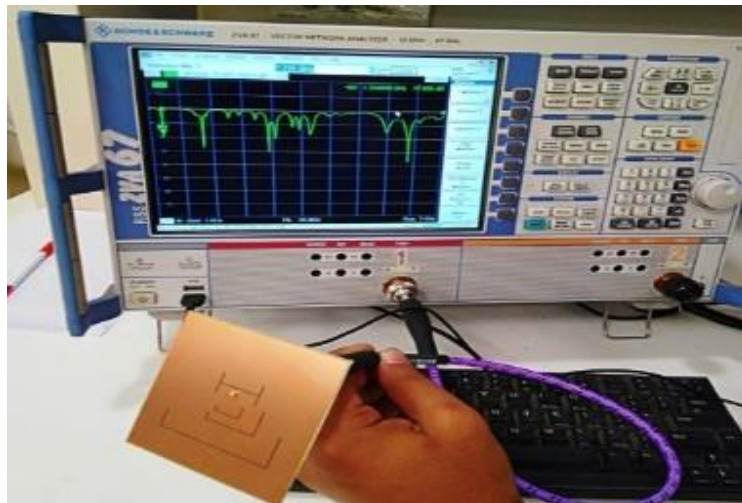


Fig 13. Antenna experimental testing

The simulation result appears a good reflection coefficient at desired frequencies 2GHz, 3.7GHz and 5.8 GHz below -20 dB as shown inFigure-14.

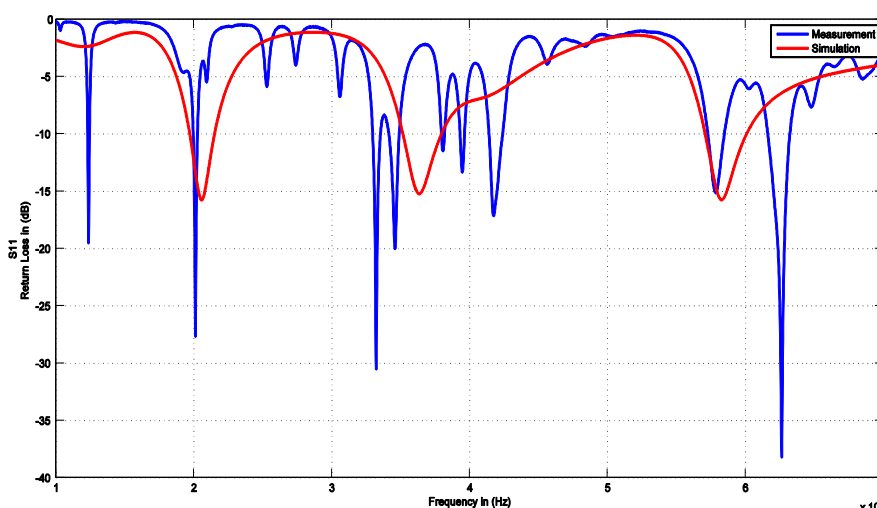


Fig 14. Simulated and measured S_{11} of the antenna

V. Rectifier design and results

The goal of an RF energy harvesting system is to convert the receiving RF energy from RF radiated surrounding waves into DC power [13- 20]. Such harvesting system as consists of a receiving antenna, band pass filter, RF-DC rectifier and load as shown in Figure-15. The receiving antenna is modeled as a simple 50Ω resistor at the desired frequencies. The chosen band pass filter topology is a variant of L- network filter in order to increase the bandwidth [15-18]. The RF-DC rectifier circuit is using full wave rectifier [Greinacher]. The schottky diode HSMS-2850 is used to verify the rectifier. This diode has a good characteristic of low forward voltage as shown Figure-16. The Advanced design system (ADS 2014) software from Agilent Technologies is used to simulate the RF harvesting system. The selected three bands 2 GHz, 3.7 GHz and 5.8 GHz have multi-band and high reflection coefficient S_{11} . Collect high power will lead to high conversion efficiency is depend on input power to the RF-DC rectifier circuit, wherefore selected three bands to obtain the highest reflection coefficient as shown in Figure-17.

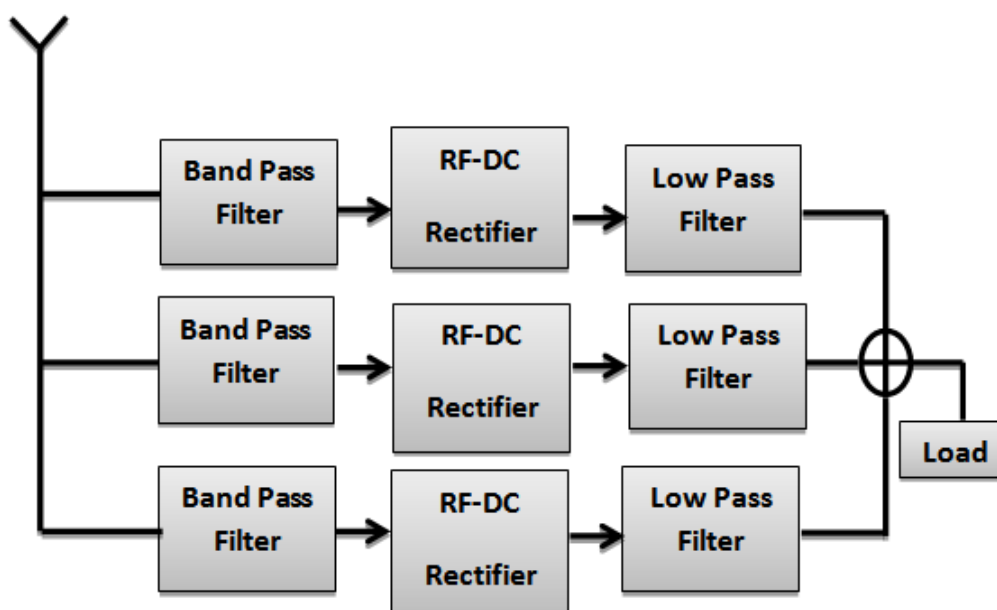


Fig 15. Multi-band RF harvesting system block diagram

Table no 3: The comparison between individual antennas and proposed antenna with respect to reflection coefficients.

Antenna	Frequency=2GHz	Frequency=3.7GHz	Frequency=5.8GHz
Individual Antenna	S(1,1) = -40.1587 dB	S(1,1) = -40.1501 dB	S(1,1) = -37.5115 dB
Proposal Antenna	S(1,1) = -22.0170 dB	S(1,1) = -21.6310 dB	S(1,1) = -24.6160 dB

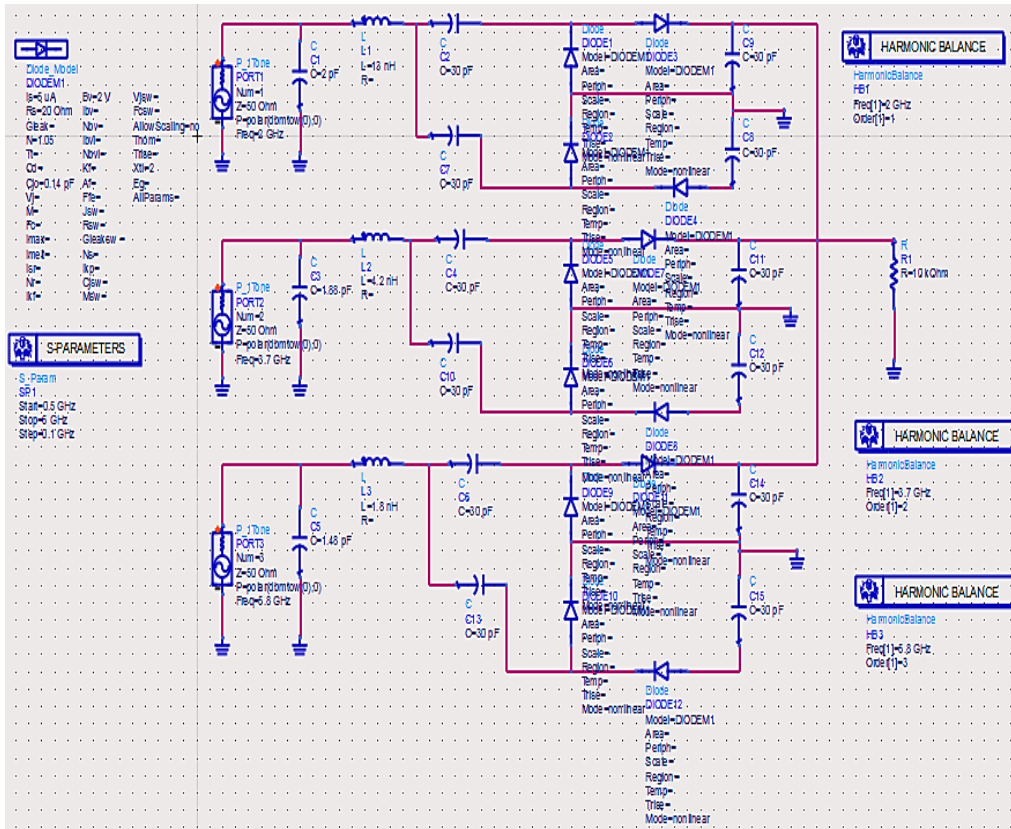


Fig 16. Full wave rectifier for three bands of proposed antenna

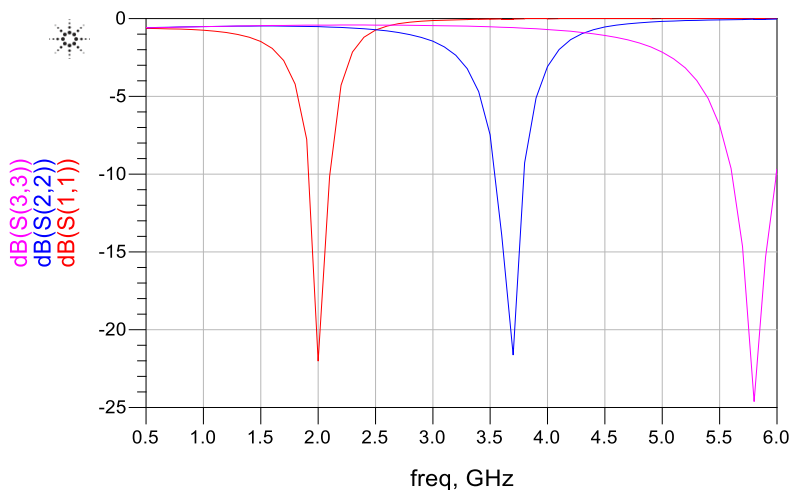


Fig 17. Magnitude of S11 for Full rectifier harvester

In the Table no3, although the values of reflection coefficients S_{11} of the three bands in individual antennas have the better magnitudes than the values which produces from the proposed antenna but the proposed antenna has many advantages more than the individual antennas such as multi band antenna can collect more energy from more one frequency 2 GHz ,3.7GHz and 5.8GHz not only one frequency at a time as individual antenna, also the proposed antenna is smaller which is very important since the smaller size antenna is much suitable to integrate in compact systems. Then more collected energy from multi-band frequency and small antenna dimensions are the desired aim of this paper.

VI. Conclusion

The geometry of the proposed antenna designed to collect a large amount of RF signals from different communication frequencies with acceptable reflection coefficients is presented. Also, we reviewed the RF-DC rectifier circuit using full wave rectifier (Greinacher) by using the advanced design system (ADS 2014) software from Agilent Technologies and to simulate the RF harvesting system. The proposal antenna has been fabricated by PCB technique and tested by vector network analyzer on FR4 double sided PCB material. The data of measurement illustrate good design for collecting large amount of power from several communication bands by using full wave rectifier circuit. Using this proposed antenna can be recommended because of its ease of fabrication, high total gain, having low size.

References

- [1]. E. Thakur, N. Jaglan, S. D. Gupta, and B. K. Kanaujia, "A Compact notched UWB MIMO antenna with enhanced performance" *Progress In Electromagnetics Research C*, vol. 91, pp. 39-53, 2019.
- [2]. M.-C. Tang, Z. Wu, T. Shi, and R. W. Ziolkowski, "Dual-band, linearly polarized, electrically small Huygens dipole antennas," *IEEE Trans. Antennas Propag.*, vol. 67, pp. 37-47, Jan. 2019.
- [3]. J. Ouyang, Y.M. Pan, and S. Y. Zheng, "Center-fed unilateral and pattern reconfigurable planar antennas with slotted ground plane," *IEEE Trans. Antennas Propag.*, vol.66, pp. 5139-5149, Oct. 2018.
- [4]. Mansoul A and Seddiki ML, "Multiband reconfigurable Bowtie slot antenna using switchable slot extensions for Wi-Fi, WiMAX, and WLAN applications," *Microwave and Optical Technology Letters*, vol.60, pp. 413-418, 2018.
- [5]. Tang, H. Wang, T. Deng, and R. W. Ziolkowski, "Compact planar ultra wide band antennas with continuously tunable independent band-notched filters," *IEEE Transactions on Antennas and Propagation*, vol. 64, pp. 3292-3301, Aug. 2016.
- [6]. Jaglan, S. D. Gupta, B. K. Kanaujia, and S. Srivastava, "Design and development of efficient EBG structures based band notched UWB circular monopole antenna," *Wireless Personal Communication, Springer*, May 2017.
- [7]. Ali, W. A. E., and R. M. A. Moniem, "Frequency reconfigurable triple band-notched ultra-wideband antenna with compact size," *Progress In Electromagnetics Research C*, vol. 73, pp. 37-46, 2017.
- [8]. Thavakumar S and Susila M, "Design of an internal multi-resonant PIFA antenna for mobile telecommunication networks," *Optical and Microwave Technologies*, vol.46, pp. 203-209, 2018.
- [9]. Costanzo, A. Romani, D. Masotti, N. Arbizzani, and V. Rizzoli, "RF/baseband co-design of switching receivers for multiband microwave energy harvesting," *Sens. Actuat. A, Phys.*, vol.179, pp.158-168, 2012.
- [10]. Kunwar A et al., "Inverted L-slot triple-band antenna with defected ground structure for WLAN and WIMAX applications," *International Journal of Microwave and Wireless Technology*, vol. 9, pp. 191-196, 2017.
- [11]. Pozar, D. M. and D. H. Schaubert, "Scan blindness in infinite phased arrays of printed dipoles," *IEEE Trans. Antennas Propag.*, vol. 32, pp. 602-610, 1984.
- [12]. Ojaroudi, N. and M. Ojaroudi, "Small square monopole antenna having variable frequency bandnotch operation for UWB wireless communications," *Microwave and Optical Technology Letters*, vol. 54, pp. 1994-1998, 2012.
- [13]. Naresh Kumar Darimireddy, R. Ramana Reddy, and A. Mallikarjuna Prasad, "Design of triple-double U-slot patch antenna for wireless applications" *Journal of Applied Research and Technology*, vol. 13, pp. 526-534, October 2015.
- [14]. Sainati, R. A., CAD of Micro Strip Antenna for Wireless Applications, Artech House Inc., 1996.
- [15]. D. Masotti, A. Costanzo, P. Francia, M. Filippi, and A. Romani, "A load-modulated rectifier for RF micropower harvesting with start-up strategies," *IEEE Trans. Microw. Theory Techn.*, vol.62, no. 4, pp.994- 1004, Apr. 2014.
- [16]. H. Sun, Y. X. Guo, M. He, and Z. Zhong, "Design of a high-efficiency 2.45 GHz rectenna for low-input-power energy harvesting," *IEEE Antennas Wireless Propag. Lett.*, vol. 11, pp. 929-932, 2012.
- [17]. K. F. Lee, S. L. Steven Yang, A. A. Kishk, and K. M. Luk, "The versatile U- slot patch antenna," *IEEE Antennas and Propagation Magazine*, vol. 53, pp. 71-88, 2010.
- [18]. E. Falkenstein, M. Roberg, and Z. Popovic, "Low-power wireless power delivery," *IEEE Trans. Microw. Theory Techn.*, vol. 60, no. 7, pp. 2277-2286, Jul. 2012.
- [19]. C. A. Balanis, *Antenna Theory: Analysis and Design*, 3rd ed. Hoboken, NJ, USA: Wiley, 2005.
- [20]. Cion O Mathuna, Terence O Donnell, and James Rohan, "Energy scavenging for long-term deployable wireless sensor networks," *Elsevier Talanta*, vol. 75, pp. 613-623, 2008.
- [21]. N. M. Din, C. K. Chakrabarty, A. Bin Ismail, and W.-Y. Chen, "Design of RF energy harvesting system for energizing low power devices" *Progress In Electromagnetics Research*, vol. 132, pp. 49-69, 2012.
- [22]. Sudou, H. Takao, K. Sawada, and M. Ishida, "A novel RF induced DC power supply system for integrated ubiquitous micro sensor devices," *International Solid-State Sensors, Actuators and Microsystems Conference*, pp. 907-910, 2007.
- [23]. Hamid Jabbar, Young. S. Song, and Taikyeong Ted.Jeong, "RF energy harvesting system and circuits for charging of mobile devices" *IEEE Transactions on Consumer Electronics*, vol. 56, pp. 247-253, 2010.
- [24]. Ghosh, C. K., B. Mandal, and S. K. Parui, "Mutual coupling reduction of a dual-frequency microstrip antenna array by using U-shaped DGS and inverted U-shaped microstrip resonator," *Progress in Electromagnetics Research C*, vol. 48, pp. 61-68, 2014.

Ahmed Samir. " Design of a Multi-Band U-Slot Microstrip Patch Antenna." *IOSR Journal of Electronics and Communication Engineering (IOSR-JECE)* 14.6 (2019): 29-39.